



SOIL-FOUNDATION-STRUCTURE INTERACTION EFFECTS ON MODEL BUILDINGS WITHIN A GEOTECHNICAL CENTRIFUGE

H. B. Mason¹, Z. Chen², K. C. Jones¹, N. W. Trombetta³, J. D. Bray⁴, T. C. Hutchinson⁵, C. Bolisetti⁶, A. S. Whittaker⁷, B. Y. Choy⁸, B. L. Kutter⁹, and G. L. Fiegel¹⁰

ABSTRACT

This paper describes a geotechnical centrifuge test that is part of a study investigating soil-foundation-structure interaction effects in dense urban environments. Two prototypical structures, a three-story building on spread footings and a nine-story building on a three-story basement, are located sufficiently far apart to be considered isolated from each other. The results show that kinematic soil-foundation-structure interaction is important for structures founded on deep, stiff basements. Additionally, acceleration amplification factors from the ground to roof levels of these buildings are under two and during intense motions, more than 50% of the roof drift of the shallow spread footing-supported structure is attributed to foundation movements. For lower intensity motions, the foundation movements only contribute approximately 20% of the roof drift.

Introduction

The authors are participating in a collaborative research project to understand soil-foundation-structure interaction (SFSI) in dense urban environments (Chen et al. 2010, Mason et al. 2010a). A series of seven centrifuge tests is being performed using the large geotechnical centrifuge at the University of California at Davis, which is part of the George E. Brown, Jr. Network for Earthquake Engineering Simulation (NEES, www.nees.org) funded by the National Science Foundation. The results of the centrifuge tests, when coupled with well-calibrated numerical models, will be employed to develop guidance for incorporating SFSI effects into seismic building codes and procedures for performance-based seismic design and assessment.

This paper focuses on results from the project's baseline test that examines two prototypical structures founded a significant distance apart (i.e., two isolated structures). One

¹ Graduate Student Researcher, Dept. of Civil & Environmental Eng., UC Berkeley, CA 94720

² Postdoctoral Researcher, Dept. of Structural Eng., UCSD, La Jolla, CA 92093

³ Graduate Student Researcher, Dept. of Structural Eng., UCSD, La Jolla, CA 92093

⁴ Professor, Dept. of Civil & Environmental Eng., UC Berkeley, CA 94720

⁵ Associate Professor, Dept. of Structural Eng., UCSD, La Jolla, CA 92093

⁶ Graduate Student Researcher, Dept. of Civil, Structural and Environmental Eng., University of Buffalo, NY 14260

⁷ Professor, Dept. of Civil, Structural and Environmental Eng., University of Buffalo, NY 14260

⁸ Graduate Student Researcher, Dept. of Civil & Environmental Eng., UC Davis, CA 95616

⁹ Professor, Dept. of Civil & Environmental Eng., UC Davis, CA 95616

¹⁰ Professor, Dept. of Civil & Environmental Eng., Cal Poly – San Luis Obispo, CA 93407

structure is a three-story, steel, moment-frame structure founded on spread footings. The other structure is a nine-story, steel, moment-frame structure founded on a three-story basement. Scale models of both structures are placed in centrifuge container on soil that represents a 29.5 m deep deposit of dry, dense Nevada sand. Models of both buildings are shaken by a sequence of seventeen ground motions. Accelerometers, displacement gauges, and strain gauges record the behavior of the soil and structures during the test sequence.

Results from the test illustrate (1) the kinematic soil-foundation-structure interaction observed during earthquake shaking, (2) the amplification of acceleration as the waves propagate through the soil and into the structure, (3) the structural nonlinearity and damage observed, and (4) the factors that contributed to the total measured story drift (e.g., foundation rocking and structural flexure).

Background

Kutter (1995) states that the objective of centrifuge testing "...is to establish in a reduced scale model identical strength, stiffness and stress as that which exists in a much larger prototype." The length dimensions of the model are scaled to be $N=55$ times smaller than the prototype and the centrifugal acceleration was scaled to be $N=55$ times larger than earth's gravity to achieve model similitude. Other important scaling factors used in Test-1 are discussed in Mason et al. (2010a). In this paper, all measurements are given in the prototype scale, unless otherwise stated.

Figure 1 presents schematics of the soil deposit and structural models. The two model buildings are single bay steel, moment-frame structures. A single-story model founded on spread footings, herein referred to as MS1F_SF80, is used to represent a three-story prototype building. A three-story model founded on a single story basement, herein referred to as MS3F_B, is used to represent a nine-story prototype building founded on a three-story deep basement. Details of the design of these models may be found in Chen et al. 2010. The soil model is constructed with dry, pluviated Nevada Sand with a relative density of approximately 80%. Horizontal earthquake shaking is imposed in the longitudinal direction only. Accelerometers measure the accelerations during the earthquake motion and are located within the soil, on the soil surface, on the foundations, and on the structures. Both vertical and horizontally oriented accelerometers are used, with horizontal accelerometers placed both parallel and orthogonal to the direction of shaking. Displacement transducers measure the transient and permanent displacement caused by the earthquake motion. They are located on the soil surface (to measure settlement), on the foundations (to measure settlement and rotation), and horizontally on the structures (to measure drift). High elongation strain gauges measure strain in the beams and columns and are used to characterize the level of nonlinearity of the members.

Seventeen modified recorded ground motions were used to shake the base of the soil container (see Mason et al. 2010a and Mason et al. 2010b for discussions on their details). In this paper, two ground motions are highlighted: the Saratoga-West Valley College motion recorded in the 270° direction during the 1989 Loma Prieta earthquake (herein referred to as WVC_L), and the Joshua Tree motion recorded in the 090° direction during the 1992 Landers earthquake (herein referred to as JOS_L_2). The WVC_L motion is a near-fault motion (Bray et al. 2009) of higher-intensity with a base maximum horizontal acceleration (MHA) of 0.24 g and a base maximum horizontal velocity (MHV) of 33 cm/sec. The JOS_L_2 motion is an "ordinary" motion of lower-intensity with a base MHA of 0.06 g and a base MHV of 9 cm/sec. Figure 2 shows the acceleration-time series for these two motions recorded at the base during Test-1.

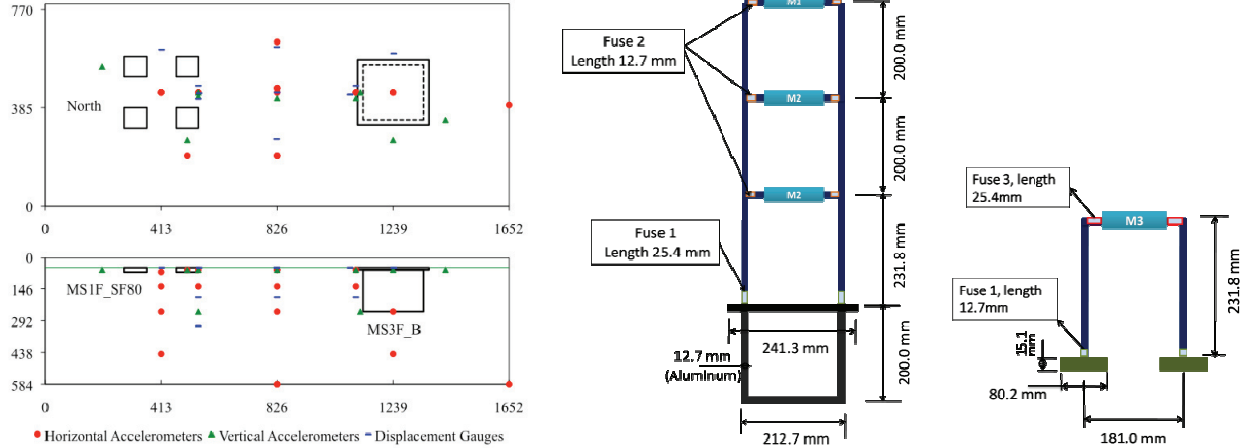


Figure 1. Elevation and plan views of the centrifuge model and structural models used for Test-1 (model scale, units in mm)

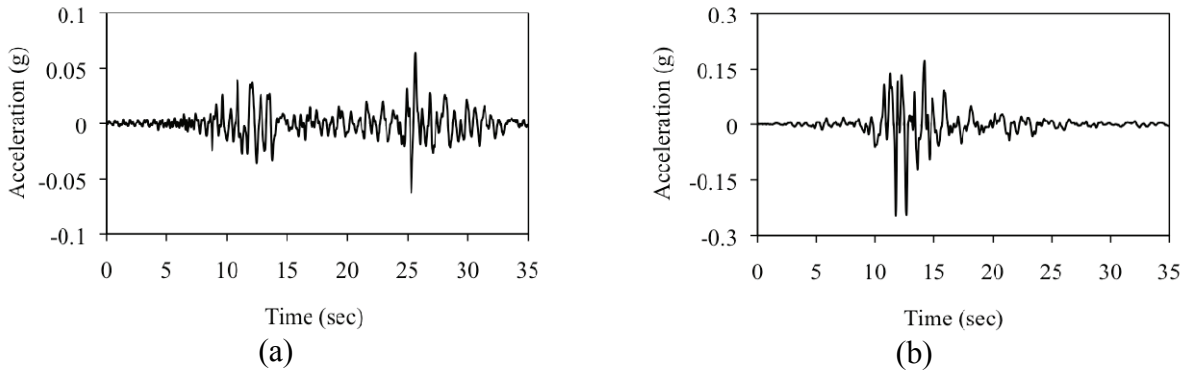


Figure 2. Acceleration-time series recorded at the base during Test-1 for: (a) the JOS_L_2 motion, and (b) the WVC_L motion.

Results

Kinematic Interaction

SFSI effects are usually subdivided into inertial interaction and kinematic interaction. The former results from the interaction of the inertial forces that develop in the structure with the supporting soil. Kinematic interaction on the other hand is caused by a relatively rigid foundation being located in a relatively compliant soil layer. The earthquake motions near the foundation tend to deviate from those recorded far away from the structure. This section focuses on kinematic interaction effects caused by the three-story basement of the MS3F_B structure.

Kinematic interaction is usually subdivided into three sub-phenomena: (1) base slab averaging, (2) embedment effects, and (3) wave scattering effects (Stewart et al. 1998). Base slab averaging arises because "...an assemblage of stiff foundation elements located on or in soil moves as a constrained body. Since free-field motions are spatially and temporally incoherent, motions on surface foundations are filtered with respect to the free-field motions" (Stewart 2000). Base slab averaging reduces the translational motion of the foundation relative to the translational motion in

the free-field. However, torsional motion and rocking of the foundation are introduced.

In nature, seismic wave incoherence is introduced because of the heterogeneity of the geologic materials that the seismic waves are traveling through as well as the fault rupture characteristics. However, in centrifuge testing, the seismic waves are introduced as vertically propagating horizontal shear waves, and the soil is relatively uniform compared to a realistic geologic profile. Incoherence in centrifuge testing is introduced because of artificial boundary conditions, namely, waves reflecting off the sides of the container. The incoherence of seismic waves in centrifuge tests may be less than in the field, and base-slab averaging effects may be masked. Embedment effects are associated with the fact that the seismic waves usually amplify as they propagate upwards from the rock below to the ground surface. The input motion that the bottom of a foundation experiences is generally smaller than the surface free-field motion. Embedment effects are important for deep basements. Seismic wave scattering occurs at the edges of the foundations, which causes wave incoherence and reduces the amplitude of the foundation input motion in the high frequency range.

It is instructive to examine the acceleration-time series of the earthquake ground motions recorded at different locations both within the soil and the foundation to examine kinematic interaction. Figure 3 shows acceleration-time series for the JOS_L_2 and WVC_L ground motions. These figures are windowed to show select portions of the strong shaking, which correspond to 8 to 11 sec (Figure 3a) and 24 to 27 sec (Figure 3b) for the JOS_L_2 motion, and 10 to 13 sec (Figure 3c) for the WVC motion. The top plots on Figure 3 show the comparison of the free-field and foundation motions. The term free-field identifies a location far enough away from the structures such that the earthquake waves are not significantly affected by that structure. In this case, the free-field motion is recorded at the soil surface in the center of the container (as far as possible from the two structures located in the box to limit wave scattering interference). The foundation motion is recorded by an accelerometer located on the top of the foundation of the MS3F_B structure. The bottom plots of Figure 3 show a comparison of the “in basement” recording and the “in soil” recording. The “in soil” recording is taken at a depth of 4.9 m and the “in basement” recording is taken at a depth of 5.6 m (both depths measured relative to the soil surface). The “in soil” accelerometer is located directly adjacent to the basement, while the “in basement” measurement is physically attached to the basement. Even though the “in basement” and “in soil” accelerometers are not located at the same depth, they provide a qualitative means for examining embedment effects associated with kinematic interaction.

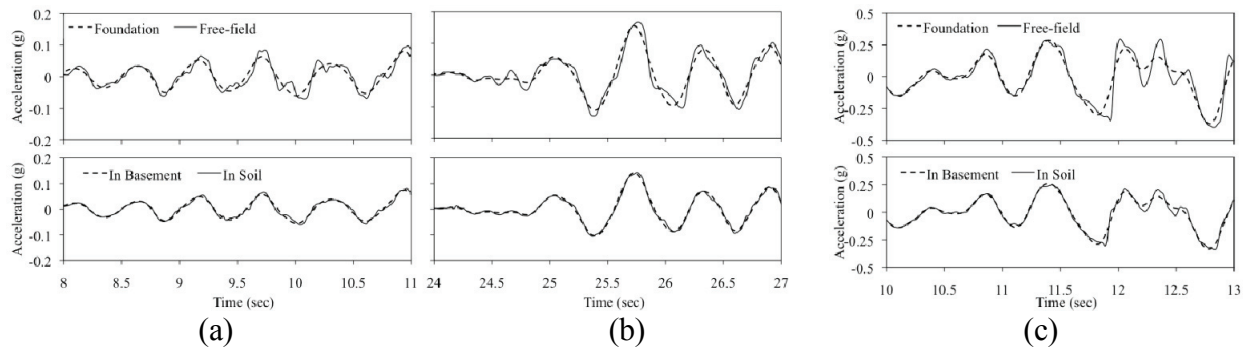


Figure 3. Acceleration-time series plots for (a) the JOS_L_2 ground motion from 8 to 11 sec, (b) the JOS_L_2 ground motion from 24 to 27 sec, and (c) the WVC_L motion from 10 to 13 sec (see Figure 2 for time references)

The top plots of Figure 3 highlight kinematic interaction effects and especially base-slab averaging. The foundation motion does not contain the same high-frequency content as the free-field motion. By comparing the top and bottom rows of data in Figure 3, one notes that the foundation translates as a rigid body in the relatively compliant soil layer.

The bottom plots of Figure 3 show that embedment effects are not important at mid-height of the basement. There are insignificant differences between the “in basement” and “in soil” accelerometer recordings at this depth (though it should once again be noted that these accelerometers are not at the exact same depth).

Amplification of Acceleration

Figure 4 presents profiles of normalized peak horizontal acceleration over the depth of the soil column and over the height of the one- and three-story structures. Data are presented for the same low-and high-amplitude motions, namely JOS_L_2 and WVC_2. The accelerations are normalized by the peak acceleration at the bottom of the soil column (base input) and are not recorded at the same instant of time. The values of normalized peak acceleration are obtained by filtering the model-scale acceleration time series at a frequency of 1000 Hz. The free-field data (denoted by FF in the legends) are obtained from accelerometers in the soil column away from the two buildings.

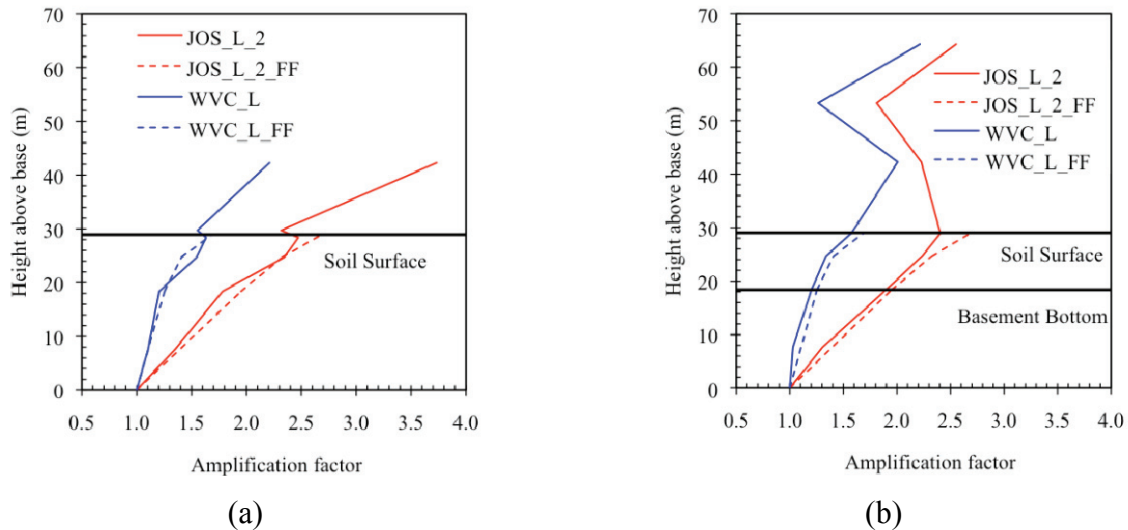


Figure 4. Profiles of peak horizontal acceleration amplification factor for: (a) the three-story structure, and (b) the nine-story structure

The amplification of the base input motion in the soil columns beneath the structural models and in the free field is similar for both model structures. Greater amplification is evident for the low-amplitude motion, which is attributed to both the different frequency content of the input motions and modest nonlinear response of the soil for the WVC_L motion.

The amplification of the foundation motion to the roof of the one-story model is by factors of 1.7 and 1.3 for the JOS_L_2 and WVC motions, respectively, which is an expected result given the nonlinear action in the model for the higher amplitude motion. The amplification factors for the three-story model for the JOS_L_2 and WPV motions are 1.1 and 1.4, respectively.

ly. The profiles of peak floor acceleration are not linear as suggested by ASCE 7-05 but are rather influenced by second and third mode responses. The amplitudes of the peak floor accelerations are of the order of the peak acceleration at the ground floor of the model as noted by Burgos et al. (2009) and implemented in the 50% draft of the ATC-58 Guideline (ATC 2009). Each value of the amplification factor is much smaller than the value of 3 calculated using the predictive equation of Section 13.3 of ASCE-7-05 (ASCE 2005).

Observed Structural Nonlinearity and Damage

Structural damage in this study consists of material yielding in the fuse sections of the beams and columns. During the six motions that preceded JOS_L_2, both the beams and columns in MS3F_B remained elastic. In contrast, the beam fuses in MS1F_SF80 yielded during these motions; the beams in the model were replaced prior to JOS_L_2. As a result, both models were undamaged prior to this motion. Strain gage data, shown in Figure 5 for MS3F_B confirm that neither model yielded during JOS_L_2.

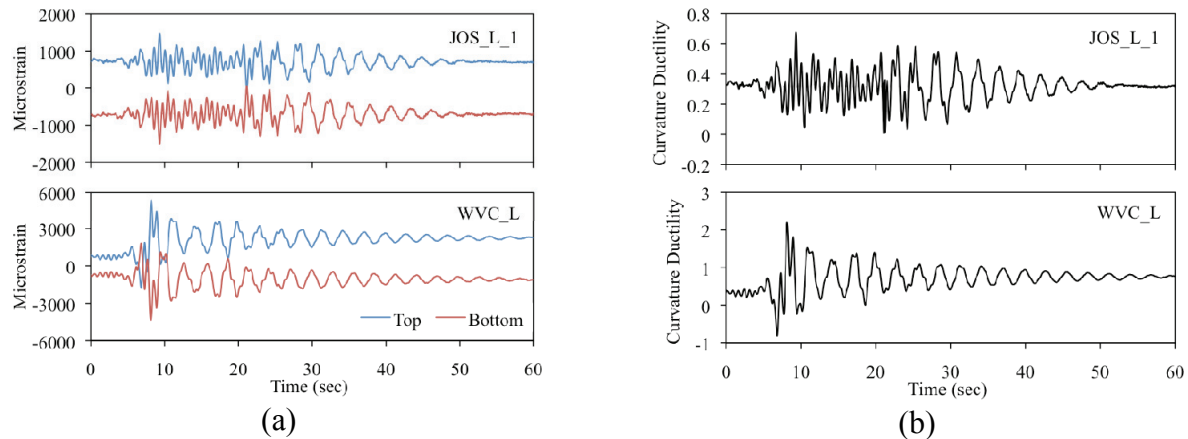


Figure 5. (a) Strain time histories (top and bottom flanges of 1st story hinge) in MS3F_B for JOS_2_L and WVC_L motion, and (b) resulting curvature ductility.

The motion SCS_L_2, which occurred between JOS_L_2 and WVC_L, did not induce in yielding of either structure. Therefore, an undamaged condition can be assumed for both models prior to WVC_L shaking. The data presented in Figure 5 show that MS3F_B yielded during shaking, as shown by the maximum curvature ductility of 2.2, and the resulting increase in residual curvature (curvature ductility at end of shaking increased from 0.33 to 0.76). Visual inspection of high-speed video data showed that small-scale yielding also occurred in the beams of MS1F_SF80. This failure was of a shear-like mode, which could not be captured by the arrangement of strain gages, as described in Chen et al. 2010. Because of the observed structural yielding in both structures, nonlinear analysis is necessary to describe fully the observed SFSI response during WVC_L.

SFSI Contributions to the Total Lateral Drift of the Buildings

Separation of story drift into components is a useful way to study SFSI (Bielak 1975; Veltetsos and Nair 1975; Luco et al. 1990; Stewart et al. 1998). For a structure-foundation system

constructed on compliant geological medium, its lateral displacements relative to the ground (in 2D) can be parsed into 3 components: (i) deformation of the superstructure, (ii) foundation translation due to soil deformation, and (iii) foundation rocking.

Structure MS3F_B

We utilize recorded acceleration data to study the histories of displacements at the roof of MS3F_B. Double integration is carried out over the acceleration-time series to obtain the displacement histories. This integration process does not recover the permanent displacement. Nonetheless, this approach is valid for this three-story model, since insignificant permanent deformation is observed. Figure 6 presents results for WVC_L. Table 1 summarizes each component of displacement at peak roof drift for JOS_L_2 and WVC_L. Based on the data presented in this table, the displacements due to foundation translation and rocking are insignificant. This is expected as this model was (i) constructed with a basement much stiffer than the superstructure, (ii) deeply embedded in the soil, and (iii) the soil was a dense sand.

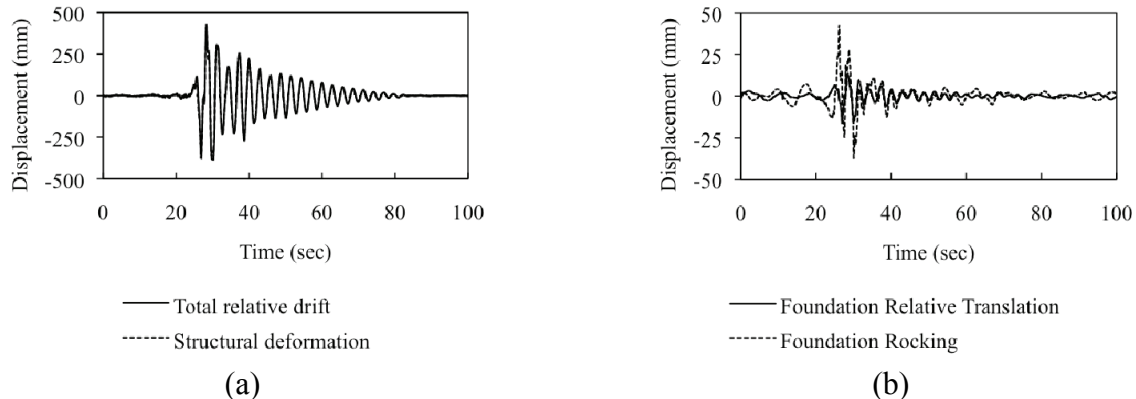


Figure 6. Time histories of total relative drift at the roof of MS3F_B and its components for the WVC event: (a) the total relative drift and the structural deformation induced drift, and (b) the drift resulting from the relative foundation translation and the drift resulting from foundation rocking.

Table 1. Drift contributions at the roof of MS3F_B under JOS_L_2 and WVC_L

JOS_L_2			WVC_L		
Displacement (mm)	Drift Ratio (%)	Contribution (%)	Displacement (mm)	Drift Ratio (%)	Contribution (%)
Δ^r 0.7	0.004	0.8	13.7	0.04	3.2
Δ^f 1.6	0.006	1.8	12.7	0.04	2.9
Δ^s 84.5	0.24	97.4	407.6	1.17	93.9
Δ^t_{\max} 86.8	0.25	100	434.0	1.25	100

Note: Δ^r – roof displacement due to foundation rocking; Δ^f – roof displacement due to foundation translation; Δ^s – roof displacement due to structural deformation; Δ^t – total roof displacement. All quantities are relative to ground.

Structure MS1F_SF80

The calculations were repeated for MS1F_SF80, and results are presented in Table 2. For this model, a significant percentage of the roof drift is attributed to foundation rocking and a smaller percentage is due to foundation translation.

Table 2. Drift contributions at the roof of MS1F_SF80 due to JOS_L_2 and WVC_L.

JOS_L_2			WVC_L		
Displacement (mm)	Drift Ratio (%)	Contribution (%)	Displacement (mm)	Drift Ratio (%)	Contribution (%)
Δ^r	10.1	0.08	16.5	86.8	0.68
Δ^f	4.8	0.04	7.8	13.8	0.11
Δ^s	46.5	0.36	75.7	76.1	0.60
Δ_{\max}^t	61.4	0.48	100	176.7	1.39

Note: the notations (Δ^r , Δ^f , Δ^s and Δ^t) are same as in Table 1.

Motion histories of rocking and foundation sliding are obtained from the LVDT displacement sensors deployed on the footings. The drifts due to foundation rocking and translation at the roof of MS1F_SP80 are shown in Figure 7. It can be seen from looking at 7(a) to 7(b) that permanent displacements accrued.

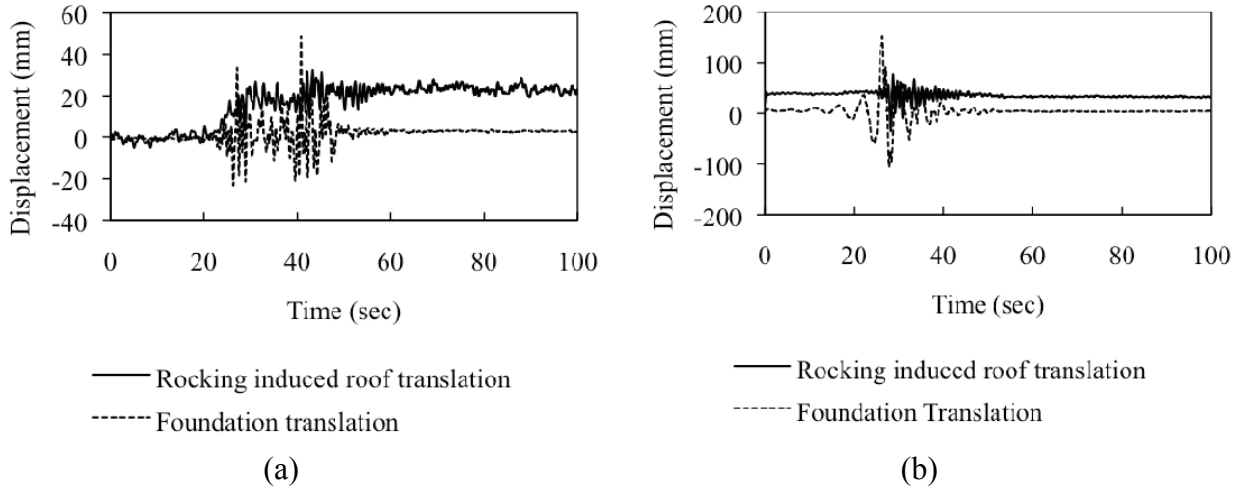


Figure 7. Time histories of foundation rocking and translation induced drift at the roof of MS1F_SP80 under two events: (a) JOS_L_2 and (b) WVC.

Conclusions

A baseline centrifuge test has been conducted examining soil-foundation-structure interaction effects for two prototypical buildings. In this test, a prototype three-story steel, moment-frame building founded on spread footings and a nine-story steel, moment-frame building founded on a three-story basement are tested. The two structures are located as far apart as possible, and are thus considered to be essentially “independent” from one another. The structures are founded on a dry, dense bed of Nevada sand. Future research will look at interaction of closely

spaced structures.

For this test, kinematic soil-structure-foundation interaction is particularly important for the nine-story structure – since it is founded on a deeply embedded, relatively rigid basement. The kinematic interaction effects are visible on zoomed-in plots of acceleration-times series – which show how the frequency-content of the motion recorded on the foundation differs from the motion recorded in the free-field. Specifically, the basement acts as a low-pass filter and reduces the high-frequency content of the ground motion.

Evaluation of the individual building response indicates that for both buildings, acceleration amplification is well below code-based calculated values, with amplification factors (ground to roof level) under 2.0, but further research is necessary to confirm how consistent this trend is. Nonlinearity in the superstructure of both model buildings is observed at predefined hinge locations. Finally, by systematically evaluating the various contributions to the total lateral displacement of the building at its roof level, one observes a clear indication of nonlinear SFSI effects for the shallow spread footing-supported building. During the higher intensity motions, more than 50% of the lateral movement of the structure is attribute to foundation displacements. For lower intensity motions, foundation movement contributes approximately 20% of the roof drift.

Acknowledgements

This material is based upon work supported by the National Science Foundation under Grant No. CMMI-0830331. Any opinions, findings, and conclusions or recommendations expressed in this material are those of the authors and do not necessarily reflect the views of the National Science Foundation. The authors gratefully acknowledge the assistance of the staff of the Center for Geotechnical Modeling at the University of California at Davis during the centrifuge testing. We would also like to acknowledge the significant contributions of members of our professional practice committee: Marshall Lew, Mark Moore, Farzad Naeim, Farhang Ostdan, Paul Somerville, and Michael Willford. Additionally, the editorial assistance of Robert Reitherman is gratefully acknowledged.

References

- American Society of Civil Engineers (ASCE), (2006). *Minimum design loads for buildings and other structures*, Reston, VA.
- Applied Technology Council (ATC) (2008). *Guidelines for seismic performance assessment of buildings: 50% draft*. Redwood City, CA.
- Bielak, J. (1975). "Dynamic behavior of structures with embedded foundations," *Earthquake Engineering and Structural Dynamics* 3, 259-274.
- Bray, J. D., Rodriguez-Marek, A., and Gillie, J. L. (2009). "Design ground motions near active faults," *Bulletin of the New Zealand Society for Earthquake Engineering* 42(1), 1-8.
- Burgos, E. A., Whittaker, A. W., Hamburger, R. O., and Huang, Y.-N. (2009). "Story drift and floor acceleration in conventional and hybrid framing systems," *Earthquake Spectra*, accepted for publication.
- Chen, Z., T. C. Hutchinson, Trombetta, N. W., Mason, H. B., Bray, J. D., Jones, K. C., Bolisetti, C., Whittaker, A. S., Choy, B. Y., Kutter, B. L., Fiegel, G. L., Montgomery, J., Patel, R. J., and Reitherman, R. K., (2010). "Seismic performance assessment in dense urban environments: evaluation of nonlinear building-foundation systems using centrifuge tests," *Fifth International Conference on Recent Advances in Geotechnical Engineering and Soil Dynamics*, May 24-29, 2010,

San Diego, CA.

- Kutter, B. L. (1995). "Recent advances in centrifuge modeling of seismic shaking," *Proceedings: Third International Conference on Recent Advances in Geotechnical Earthquake Engineering and Soil Dynamics*, April 2-7, St. Louis, Missouri.
- Luco, J., J. Anderson, and Georgevich M. (1990). "Soil-structure interaction effects on strong motion accelerograms recorded on instrument shelter," *Earthquake Engineering and Structural Dynamics* 19, 119-131.
- Mason, H. B., Bray, J. D., Jones, K. C., Chen, Z., Hutchinson, T. C., Trombetta, N. W., Choy, B. Y., Kutter, B. L., Fiegel, G. L., Montgomery, J., Patel, R. J., Reitherman, R. K., Bolisetti, C., and Whittaker A. S., (2010a). "Earthquake input motions and seismic site response in centrifuge tests examining SFSI effects," *Proceedings of the Fifth International Conference on Recent Advances in Geotechnical Earthquake Engineering and Soil Dynamics*, May 24-29, San Diego, CA.
- Mason, H. B., Kutter, B. L., Bray, J. D., Wilson, D. W., and Choy B. Y., (2010b). "Earthquake motion selection and calibration for use in a geotechnical centrifuge," *Proceedings of the Seventh International Conference on Physical Modelling in Geotechnics*, June 28-July 1, Zurich, Switzerland.
- Stewart, J. P. (2000). "Variations between foundation-level and free-field earthquake ground motions," *Earthquake Spectra* 16(2), 511-532.
- Stewart, J. P., Seed, R. B., and Fenves, G. L. (1998). *Empirical evaluation of inertial soil-structure interaction effects*, Research report no. PEER-98/07, University of California, Berkeley.
- Veletsos, A. S. and Nair, V. V. D. (1975). "Seismic interaction of structures on hysteretic foundations," *Journal of Structural Engineering* 101(1), 109-129.